A Linear Rectangular Dielectric Resonator Antenna Array Fed by Dielectric Image Guide With Low Cross Polarization

Asem S. Al-Zoubi, *Member, IEEE*, Ahmed A. Kishk, *Fellow, IEEE*, and Allen W. Glisson, *Fellow, IEEE*

***Abstract*—Design of a linear array of rectangular dielectric resonator antennas (DRAs) fed by dielectric image guide (DIG) is presented. Coupling between the DIG and the DRAs is predicted using the effective dielectric constant method. In order to achieve a specific power distribution, the power coupled to each DRA is controlled by changing the spacing between the DRAs and the DIG. Cross polarization reduction is achieved by wrapping a conducting strip around the middle of the DRA without affecting the co-polarized radiation pattern. The antenna is fabricated and tested. Good agreement between the measured and computed results is obtained.**

***Index Terms*—Dielectric image guide (DIG), dielectric resonator antenna (DRA), linear array, low cross polarization.**

I. Introduction

DIELECTRIC resonator antennas (DRAs) have been widely used in the microwave and millimeter frequency bands due to their attractive radiation characteristics. They offer several potential advantages such as small size, light weight, high radiation efficiency, wide bandwidth, low loss, and no excitation of surface waves [1]–[4]. Different shapes of DRAs such as cylindrical, hemispherical, elliptical, pyramidal, rectangular, and triangular have been presented in the literature. The rectangular-shaped DRAs offer practical advantages over cylindrical and hemispherical ones in that they are easier to fabricate and have more design flexibility.

Different mechanisms for coupling energy to the DRA are used, such as the slot aperture [5], coaxial probe [6], microstrip line [7], and dielectric image guide. A dielectric image guide (DIG) has low losses at higher frequencies, and the DRA can be considered as a truncated DIG. The fields of the fundamental modes of the DRA and DIG are similar. Advantages of the DIG are low loss at high frequencies and ease of coupling energy to the DRAs. Since the DRAs are above a ground plane, the directivity is doubled, and the DIG can be designed to support one mode only. Recently, the aperture coupled dielectric resonator antenna fed by DIG has been analyzed and designed [8], [9]. Since the slot apertures radiate on both sides, such an antenna has high back radiation. A reflector was used to reduce the back radiation [10]. However, if the DRAs can be coupled to the DIG from the same side we will significantly reduce the back radiation. The array must have a specific phase and amplitude distribution in order to maximize the gain or to reduce the sidelobe levels. Several types of feeding have been used to feed a linear array of DRAs to achieve these objectives, and dielectric image guides (DIGs) can be used efficiently since they have low losses [11]–[14].

Here, a linear DRA array fed by a DIG is presented. The effective dielectric constant (EDC) [15], [16] is used to approximate the coupling between the DIG and the DRAs. A Dolph-Chebyshev amplitude distribution is used to control the sidelobe level of the array radiation pattern. From the amplitude coefficients the separation between the DIG and each DRA is obtained. The cross polarization is reduced using two methods: (a) by inserting a metal sheet at the center of the DRA normal to the propagation direction of the wave in the DIG, or (b) by wrapping a conducting strip around the DRA at the center, which is found to be simple and more practical.

In Section II, the configuration of the DIG feed line will be discussed and results for measurements and simulation for the S parameters are compared. Coupling theory will be studied in Section III, where the coupling length, power delivered to the DRA, and the required amplitude coefficient will be obtained. In Section IV the simulated results for the S parameters and radiation patterns will be presented for 7 and 15-element DRA arrays. The results are verified experimentally for the case of the 7-element DRA array. The cross polarization suppression technique is studied in Section V.

II. Configuration of the DIG Feed Line

The dielectric image guide (DIG) is shown in Fig. 1 with $a_d = 0.9$ mm, $b_d = 5.0$ mm, and $\varepsilon_{r2} = 10.2$. In order to excite the DIG, the DIG is tapered and connected to the rectangular waveguide as shown in Fig. 1. The dimensions used are given in the caption of Fig. 1. The guided wavelength of the DIG is obtained theoretically using the effective dielectric constant method and found to be 11.75 mm. The total length of the DIG is about 21 guided wavelengths, λ_g, (the tapered parts are not included in this length). The DIG ends are tapered to achieve smooth transition between the waveguide and the DIG. The geometry is fabricated using two X-band waveguides with wall thickness of 1.27 mm and a copper sheet ground plane of

Manuscript received January 03, 2009; revised August 08, 2009. First published December 28, 2009; current version published March 03, 2010.

A. S. Al-Zoubi was with the Department of Electrical Engineering, University of Mississippi, University, MS 38677 USA. He is now with the Department of Communications Engineering, Al-Yarmouk University, Irbid 21163, Jordan (e-mail: asem@yu.edu.jo).

A. A. Kishk and A. W. Glisson are with the Department of Electrical Engineering, University of Mississippi, University, MS 38677 USA (e-mail: ahmed@olemiss.edu; aglisson@olemiss.edu).

Color versions of one or more of the figures in this paper are available online at http://ieeexplore.ieee.org.

Digital Object Identifier 10.1109/TAP.2009.2039294

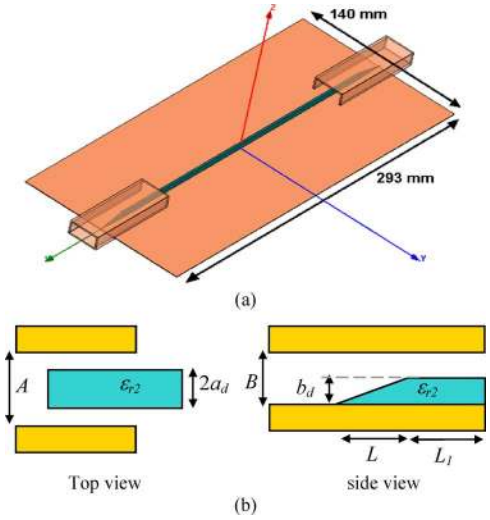

Fig. 1. Geometry of the DIG and the transition from rectangular waveguide to DIG with $A = 22.86$ mm, $B = 10.16$ mm, $L_1 = 27.5$ mm, and $L = 24.5$ mm. (a) DIG excited by a waveguide. (b) Transition from waveguide to DIG.

thickness 0.5 mm, width 140 mm, and length of 293 mm. The material used for the DIG is the RT/duroid 6010LM. The transmission coefficient and return loss for the DIG side are simulated using HFSS commercial software [17] and shown in Fig. 2. Dielectric and conductor losses are included in the simulation. From the figure it can be seen that the system with the transitions and a DIG 21 λ_g long at 10 GHz has a total insertion loss of about 1.43 dB and the reflection coefficient is less than -15 dB over the entire band.

III. Coupling Between the DRA and the DIG

The effective dielectric constant (EDC) method is used to obtain the coupling between two identical DIGs as shown in Fig. 3. Applying the boundary conditions, the following set of equations is obtained [15]:

$$b_d k_z = \frac{n\pi}{2} - \tan^{-1}\left[\frac{k_z}{\varepsilon_{r2} k_{z0}}\right] \tag{1}$$

with $k_{z0}^2 = k_0^2\left[\varepsilon_{r2} - 1\right] - k_z^2$ and $k_x^2 = \beta^2 = \varepsilon_{r2} k_0^2 - k_z^2 - k_y^2$

$$a_d k_y = \frac{m\pi}{2} - \frac{1}{2}\left\{\tan^{-1}\left[\frac{k_y}{k_{y0}}\right] + \tan^{-1}\left[\frac{D k_y}{k_{y0}}\right]\right\} \tag{2}$$

with $k_{y0}^2 = k_0^2\left[\varepsilon_{rez} - 1\right] - k_y^2$, $D = \tanh(ck_{y0})$ for odd modes and $D = \coth(ck_{y0})$ for even modes, where k_z, k_y, k_{z0}, and k_{y0} are transverse propagation constants inside and outside the guide, respectively.

The length L_c needed for complete power transfer from guide A to B in Fig. 4 is

$$L_c = \frac{\pi}{\beta_e - \beta_0} = \frac{\frac{\lambda_0}{2}}{\frac{\lambda_0}{\lambda_{ge}} - \frac{\lambda_0}{\lambda_{go}}}. \tag{3}$$

The magnitude of the coupling coefficient $|\kappa|$ between the two guides is given by

$$|\kappa| = \frac{\pi}{2L_c} = \frac{(\beta_e - \beta_o)}{2} = \frac{(k_{xe} - k_{xo})}{2}. \tag{4}$$

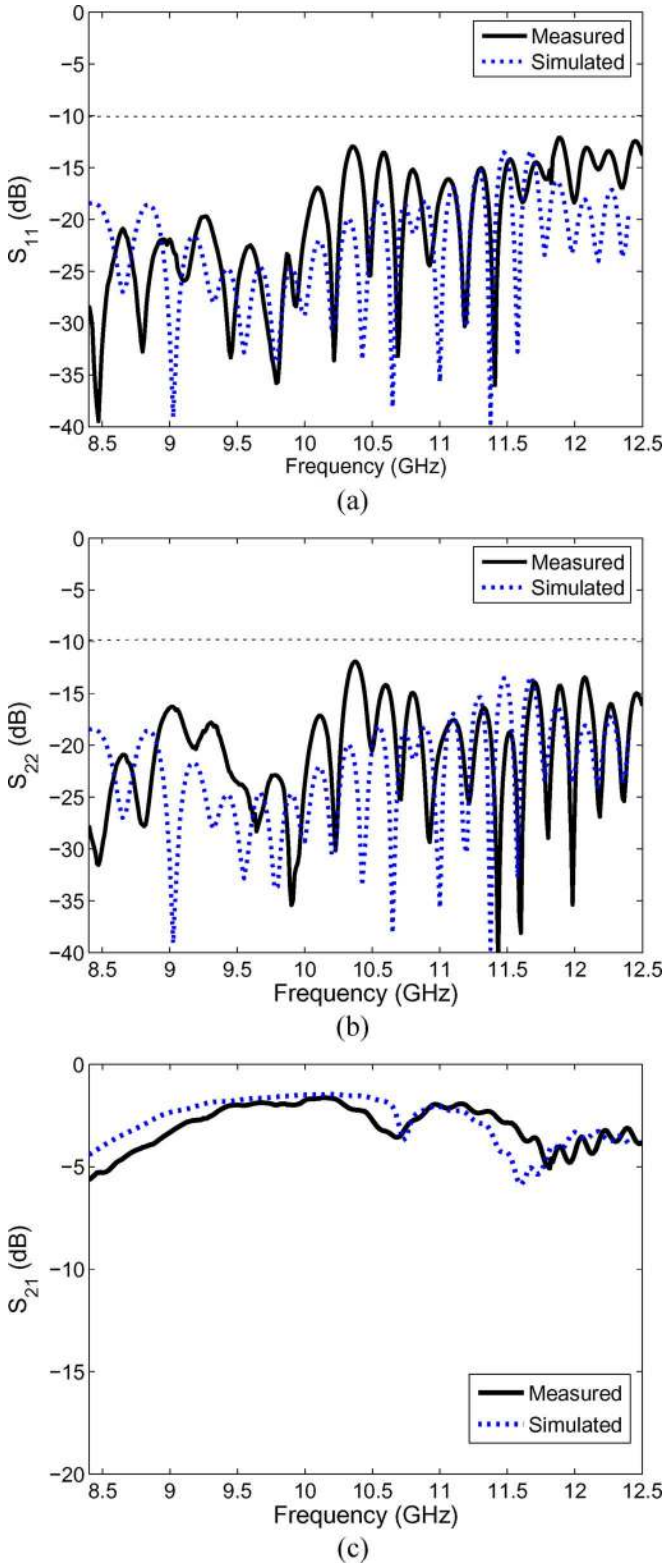

Fig. 2. S Parameters of the feeding DIG with the transitions: (a) S_{11}, (b) S_{22}, and (c) S_{21}.

For a pair of DIGs with $b_d = 5.0$ mm, $a_d = 0.9$ mm, and $\varepsilon_r = 10.2$, the propagation constants were calculated for different values of spacing $2c$. The relationship between the length L_c and the spacing $2c$ is shown in Fig. 5.

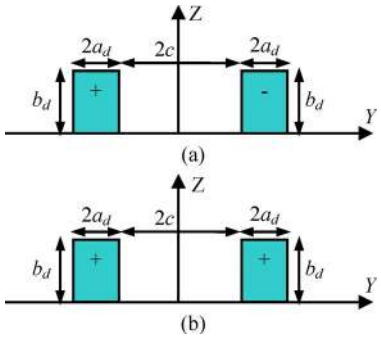

Fig. 3. Coupler configuration for (a) odd and (b) even modes.

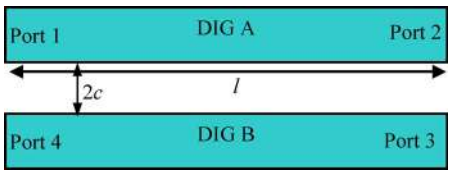

Fig. 4. Coupling section of coupled dielectric image guides.

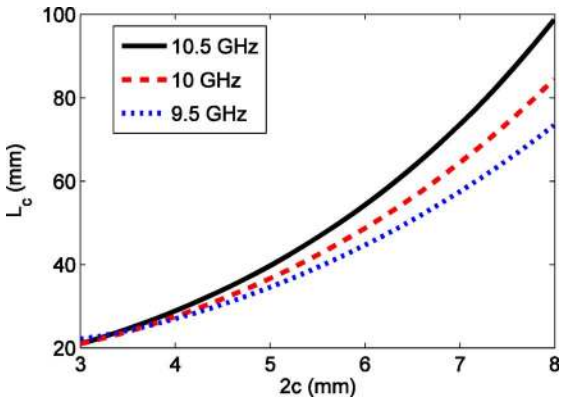

Fig. 5. Coupling length as a function of the spacing between the DIGs.

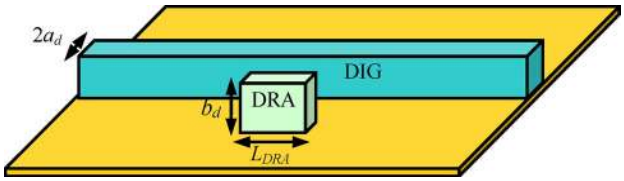

Fig. 6. Configuration of the DRA near the DIG.

The power ratio between ports 3 and 1 is

$$\frac{P_3}{P_1} = \sin^2\left(\frac{\pi l}{2L_c}\right). \tag{5}$$

If the second DIG as shown in Fig. 6 (in our case this is a DRA with the same height and width as the DIG) has a length $l = L_{\mathrm{DRA}}$, then the power coupled to the DRA is given by

$$\frac{P_{\mathrm{DRA}}}{P_{\mathrm{DIG}}} \approx \sin^2\left(\frac{\pi L_{\mathrm{DRA}}}{2L_c}\right). \tag{6}$$

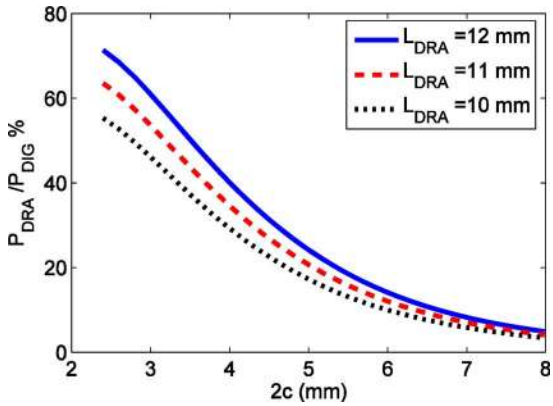

Fig. 7. Power coupled from the DIG to the DRA for different DRA lengths based on (6).

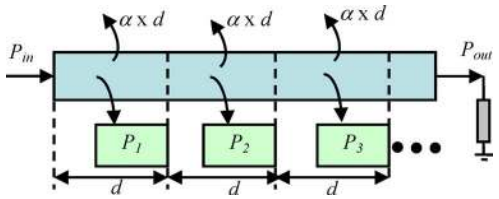

Fig. 8. DRA array fed by DIG.

Fig. 7 shows the ratio of the power of the DRA to the power of the DIG as a function of the spacing $2c$ for different DRA lengths. From the figure, as the spacing increases, the coupled power decreases. Also, as the length of the DRA increases, the coupled power increases.

The losses at each transition and the insertion and transmission losses for the system are obtained from the simulation using HFSS commercial software. The Dolph-Chebyshev amplitude distribution will be used to control the sidelobe level of the array. Fig. 8 shows the array of DRAs fed by the DIG [18]. The DIG is divided into the same number of unit cells as the number of the DRAs. Therefore, each unit cell is corresponding to a DRA. The length of the cell is equal to the spacing between the elements. Each unit cell couples a fraction of the power (P_n) from the DIG to the DRA and dissipates some energy due to conductor and dielectric losses ($\alpha \times d$). The power P_n, which is the fraction of the power coupled from the DIG into the DRA, and the loss can be written as

$$P_n = \frac{P_{\mathrm{DRA}n}}{P_{\mathrm{DIG}n}} \tag{7}$$

$$\alpha = \alpha_c + \alpha_d. \tag{8}$$

The formulas for the conductor and dielectric losses for the DIG can be found in [20].

If the output power P_{out} is zero, this means that all the input power is radiated, which means that the last DRA element absorbs all the remaining power from the DIG, but this is impractical [18]. The required power distribution is calculated from the required amplitude coefficients A_n, which is obtained using

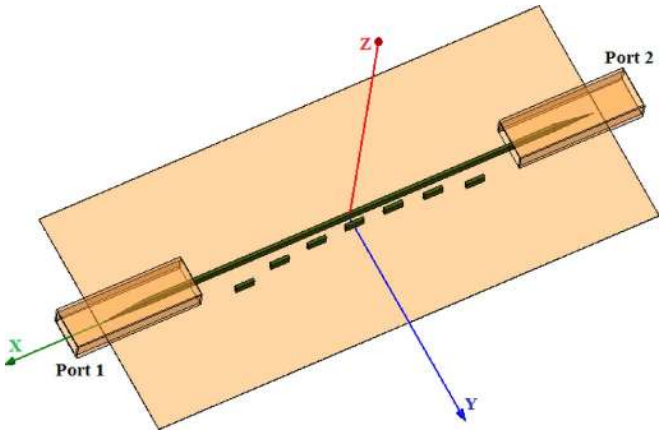

Fig. 9. Geometry of 7-element array.

TABLE I
REQUIRED AMPLITUDE AND POWER DISTRIBUTION FOR 7-ELEMENT ARRAY WITH 40 dB SIDELOBE LEVEL

N	A_n	P_{DRA}/P_{in} %	P_n %	$2c$ (mm)
1	0.1594	0.65	0.653	11.75
2	0.4794	5.86	5.95	7.32
3	0.8397	17.99	19.50	5.11
4	1.0000	25.87	34.97	3.98
5	0.8397	17.99	37.55	3.84
6	0.4794	5.86	19.67	5.10
7	0.1594	0.65	2.73	8.79

Dolph-Chebyshev amplitude distribution for a specific sidelobe level, which can be written as

$$\frac{P_{\mathrm{DRA}_n}}{P_{\mathrm{in}}} = \left(1 - \frac{P_{\mathrm{out}}}{P_{\mathrm{in}}}\right)\left(\frac{A_n^2}{\sum_{m=1}^{N} A_m^2}\right) \tag{9}$$

where P_{in} is the input power in the DIG and P_{out} is the remaining power transmitted in the DIG at the end of the DRA array. The next step is to obtain the values of the coupled power P_n. These values will be used to find the spacing between each DRA and the DIG. The equations used to obtain the power P_n can be found in [18].

IV. RESULTS AND DISCUSSION

A. 7-Element Array

The array is designed to operate at 10 GHz using 7 DRA elements of the same height and width as the DIG. The separation between elements is 23.5 mm. The DRA with $L_{\mathrm{DRA}} = 11\ \mathrm{mm}$, $a = 0.9\ \mathrm{mm}$, $b = 5\ \mathrm{mm}$, and $\varepsilon_{r1} = 10.2$ is used. The calculated dielectric and conductor losses for this DIG are obtained using the effective dielectric constant method and found to be $\alpha = 0.018\ \mathrm{Np}$.

Table I displays the coefficients A_n obtained using a Dolph-Chebyshev amplitude distribution for a sidelobe level of 40 dB, the power P_n, which is the fraction of the power coupled from the DIG into the DRA, and the required spacing $2c$ between the DRAs and the DIG. It is assumed that $P_{\mathrm{out}}/P_{\mathrm{in}} = 0.25$. The simulated geometry is shown in Fig. 9.

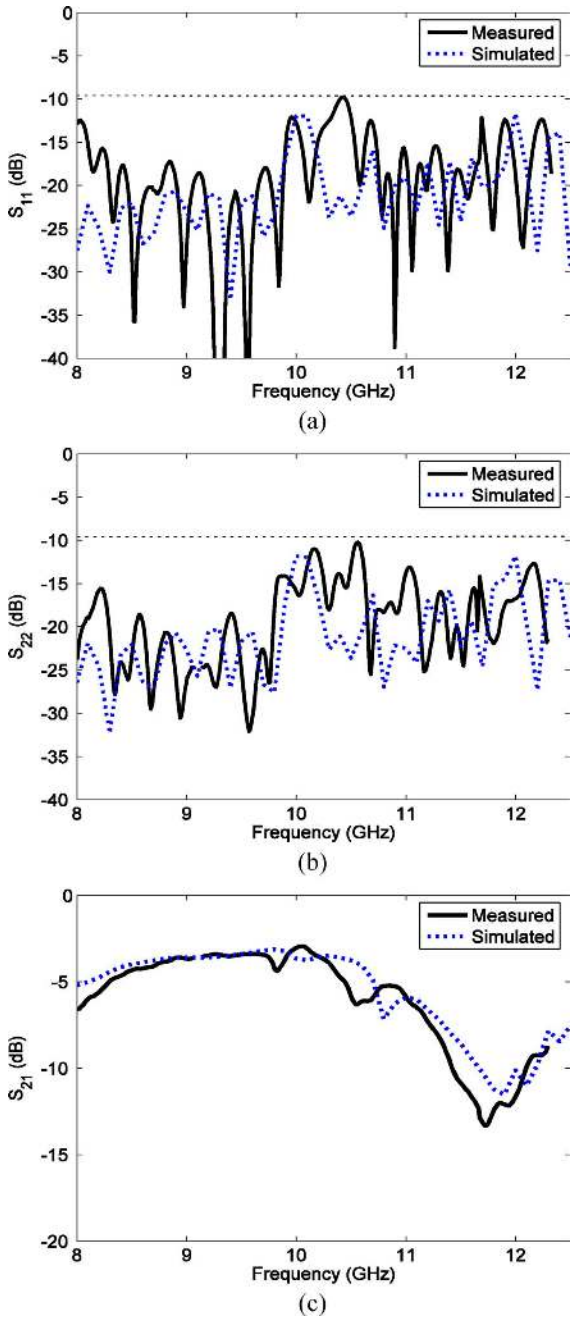

Fig. 10. Simulated and measured S parameters comparison for 7-element array (a) S_{11}, (b) S_{22}, and (c) S_{21}.

Fig. 10 shows a comparison between the measured and simulated S parameters. The transmission coefficients are almost identical, but there is a slight difference in the reflection coefficient at the input and output ports due to imperfect fabrication. It is noticed that the reflection coefficients are less than $-10\ \mathrm{dB}$ over the entire bandwidth for both the measured and simulated results.

The computed and measured radiation patterns are compared with each other as shown in Fig. 11 and show good agreement. It can be noticed that the cross polarization is very high. It can

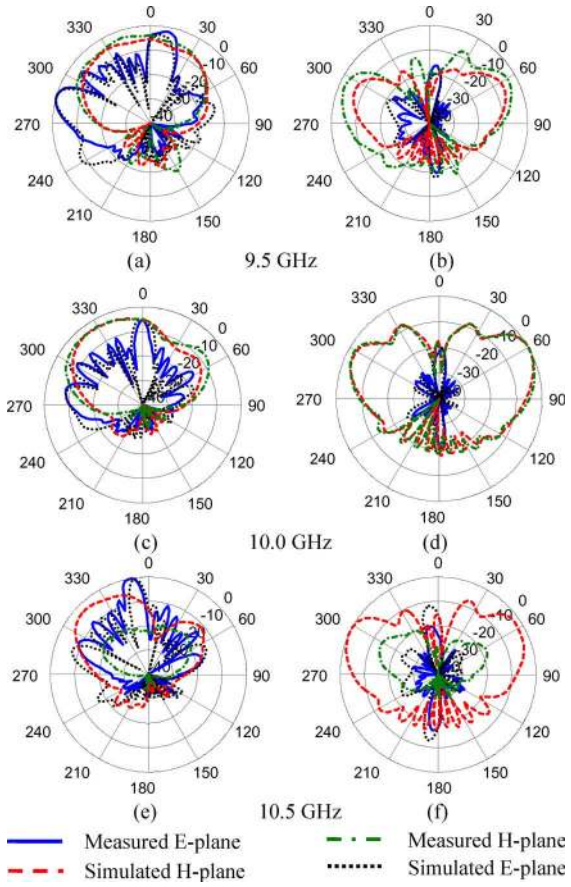

Fig. 11. Radiation patterns for the array with 40 dB sidelobe level at different frequencies. The left hand side for Co-polar patterns and the right hand side for the X-polar patterns.

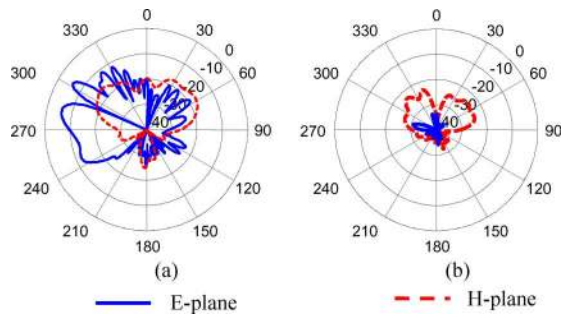

Fig. 12. Radiation patterns of the feed at 10 GHz: (a) Co-polar and (b) X-polar.

also be noticed that a strong field is radiated in the direction of the x-axis, which can be related to the direct radiation from the waveguide feed aperture. The radiation due to the feed alone is shown in Fig. 12. The gain of the antenna is measured and compared to the simulated results as shown in Table II where good agreement is observed. The computed and measured gains are the peak values of the co-polarization. The simulated radiation efficiencies are also shown in the Table II.

B. 15-Element Array

As we gained experience and confidence in the software to analyze the problem and since the radiation from the feed is strong compared to the DRA array, a larger array was designed.

TABLE II
MEASURED AND SIMULATED GAINS AND RADIATION EFFICIENCY OF THE 7-DRA ARRAY ANTENNA

Frequency (GHz)	η_{sim} %	G_{sim} (dBi)	G_{mcas} (dBi)
9.5	78.8	6.72	6.40
10.0	66.8	7.90	7.62
10.5	71.6	5.91	5.74

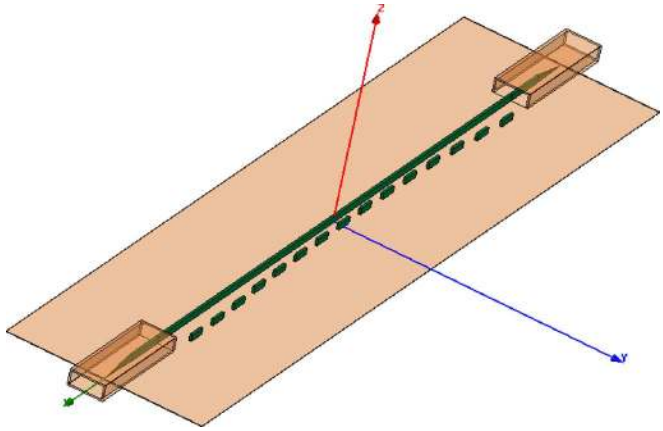

Fig. 13. Geometry of the 15-element DRA fed by DIG.

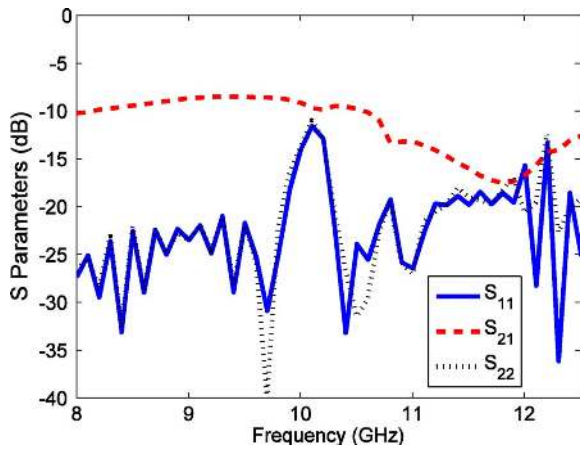

Fig. 14. Simulated S parameters for the 15-element array.

The array is designed to operate at 10 GHz with 15 DRA elements of the same height and width as the DIG. The separation between elements is 23.5 mm. DRAs with $L_{\mathrm{DRA}} = 11$ mm, $a = 0.9$ mm, $b = 5$ mm, and $\varepsilon_{r1} = 10.2$ are used.

Table III shows the coefficients A_n obtained with a Dolph-Chebyshev amplitude distribution for a sidelobe level of 40 dB, the power P_n, and the required spacing $2c$ between the DRAs and the DIG. It is assumed that $P_{\mathrm{out}}/P_{\mathrm{in}} = 0.2$. The geometry shown in Fig. 13 is simulated using HFSS. The simulated S parameters are shown in Fig. 14. It can be seen that the reflection coefficients are below -10 dB. The co-polar and cross-polar radiation patterns for this array are shown in Fig. 15 for different frequencies. The fields are normalized by the peak value at each frequency separately. It is noticed that the cross polarization at 10 GHz is very high. The simulated gain of the antenna is shown in Table IV. At 10 GHz the gain is 12.31 dBi, while for the

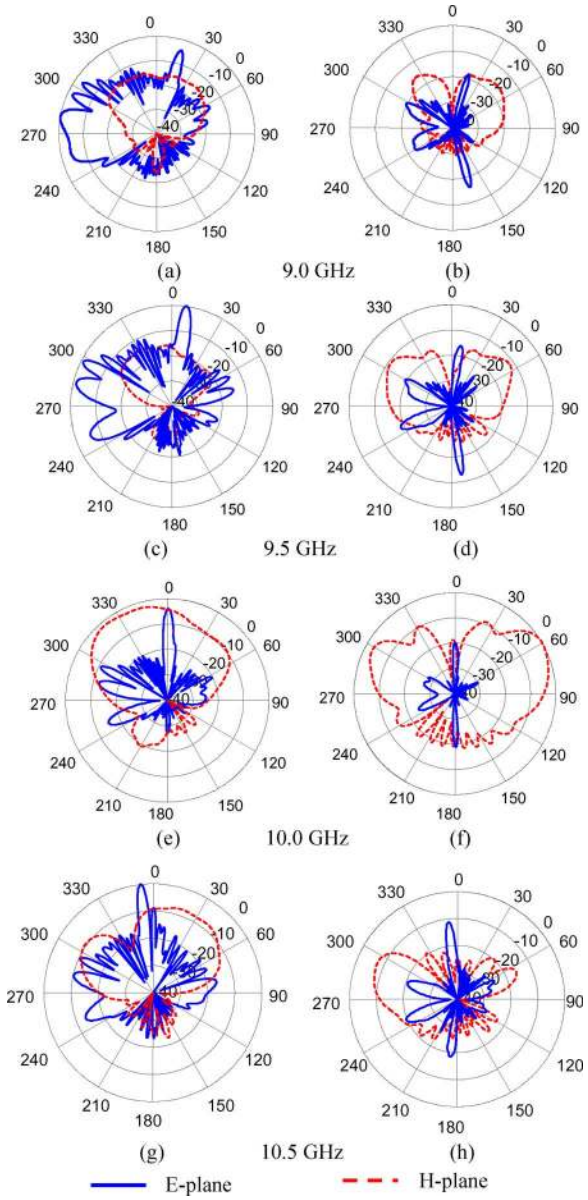

Fig. 15. Radiation patterns of the 15-element DRA array for -40 dB sidelobe level. The left hand side for co-polar patterns and the right hand side for the x-polar patterns.

7-DRA array it is 7.62 dBi. The simulated radiation efficiencies of the antenna are shown in the Table III.

V. Cross Polarization Reduction

The cross polarization is radiated due to the DIG feed and the excitation of higher order modes of the DRA. The radiated modes of the DRA are the desired TE^{y}_{111} and the undesired TE^{x}_{111} modes. The TE^{y}_{111} mode couples well to the mode excited in the DIG. The electric fields in the DIG and the DRA above a ground plane are shown in Fig. 16. Two methods are investigated to eliminate the unwanted additional modes by which the cross polarization is reduced without changing the co-polarization patterns. Since the DRA is fed along its entire length by the DIG, inserting a metal sheet at the center of the DRA perpendicular to the propagation direction will not affect the power

TABLE III
Required Amplitude and Power Distribution for 15-Element Array With 40 dB Sidelobe Level

N	A_n	P_{DRAn}/P_{in}	P_n %	$2c$ (mm)
1	0. 1124	0.162	0.163	12.5
2	0. 2055	0.542	0.547	11.9
3	0.3532	1.602	1.634	9.79
4	0.5265	3.560	3.706	8.20
5	0.7036	6.358	6.902	7.04
6	0.8577	9.448	11.06	6.17
7	0.9627	11.90	15.74	5.51
8	1.000	12.84	20.24	5.04
9	0.9627	11.90	23.62	4.75
10	0.8577	6.448	24.64	4.67
11	0.7036	6.358	22.10	4.88
12	0.5265	3.560	15.95	5.48
13	0.3532	1.602	8.580	6.64
14	0.2055	0.542	3.187	8.50
15	0.1124	0.162	0.989	10.75

TABLE IV
Simulated Gain and Radiation Efficiency of the 15-Element Array

Frequency (GHz)	η %	G_{sim} (dBi)
9.0	82.7	10.59
9.5	72.4	10.13
10.0	63.5	12.31
10.5	61.7	10.22

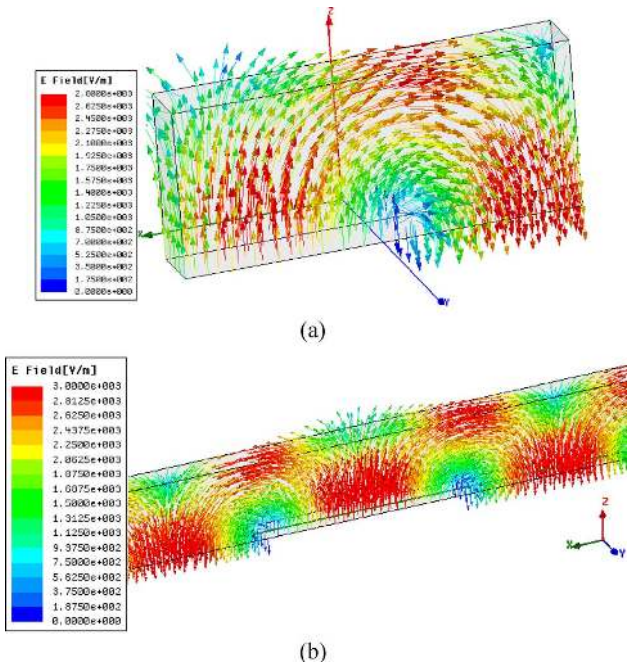

Fig. 16. Electric field vectors in the (a) DRA and (b) DIG.

distribution between the two halves of the DRA. By inserting the metal sheet at the center we eliminate the TE^{x}_{111} mode and also the TM^{z}_{111} mode.

The first method to suppress some of the undesired modes and to reduce cross-polarization is by inserting a metal sheet at the center of the DRA perpendicular to the propagation direction (perpendicular to the x-axis) as shown in Fig. 17(a) [21].

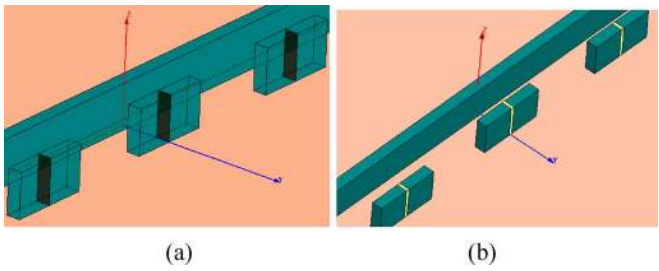

Fig. 17. Zoom view on the DIG and coupled DRAs with (a) shorting plates and (b) wrapped with a narrow conducting strip.

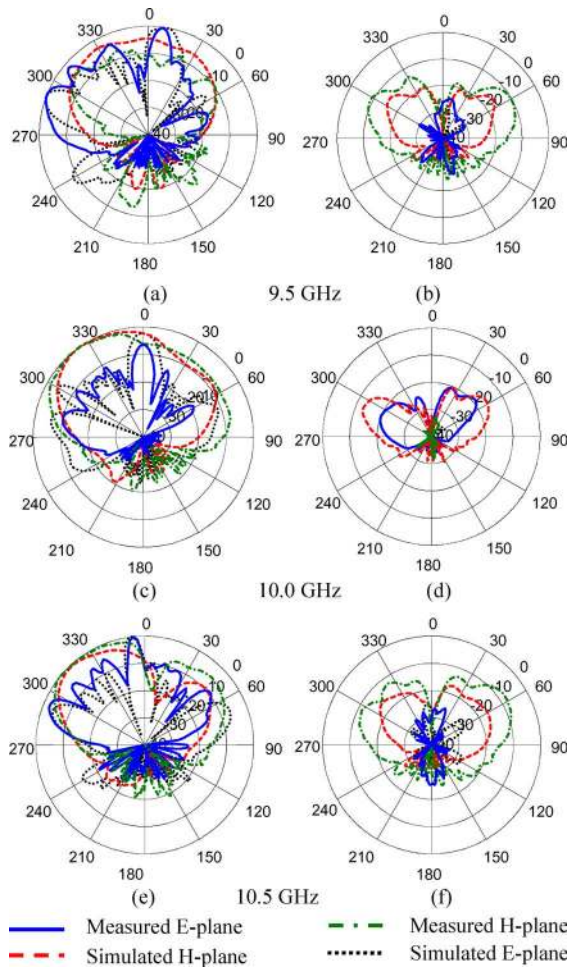

Fig. 18. Radiation patterns for the 7-element DRA array with a conducting strip around the DRA at different frequencies. The left hand side for Co-polar patterns and the right hand side for the X-polar patterns.

TABLE V
MEASURED AND SIMULATED GAINS OF THE 7-DRA ARRAY ANTENNA WITH CONDUCTING STRIPS AROUND THE DRAS

Frequency (GHz)	η %	G_{sim} (dBi)	G_{meas} (dBi)
9.5	72.2	6.05	5.93
10.0	64.6	7.61	7.02
10.5	69.7	5.76	5.68

The reduction in cross polarization is about 25 dB [20]. The results of this case are removed for brevity. This method requires splitting the DRA and gluing the conducting plate between the two halves of the DRA. The second method, which is easier and more practical to implement, is to wrap a narrow conducting strip around the DRA at the center as shown in Fig. 17(b). The cross polarization level is reduced about 20 dB in this case.

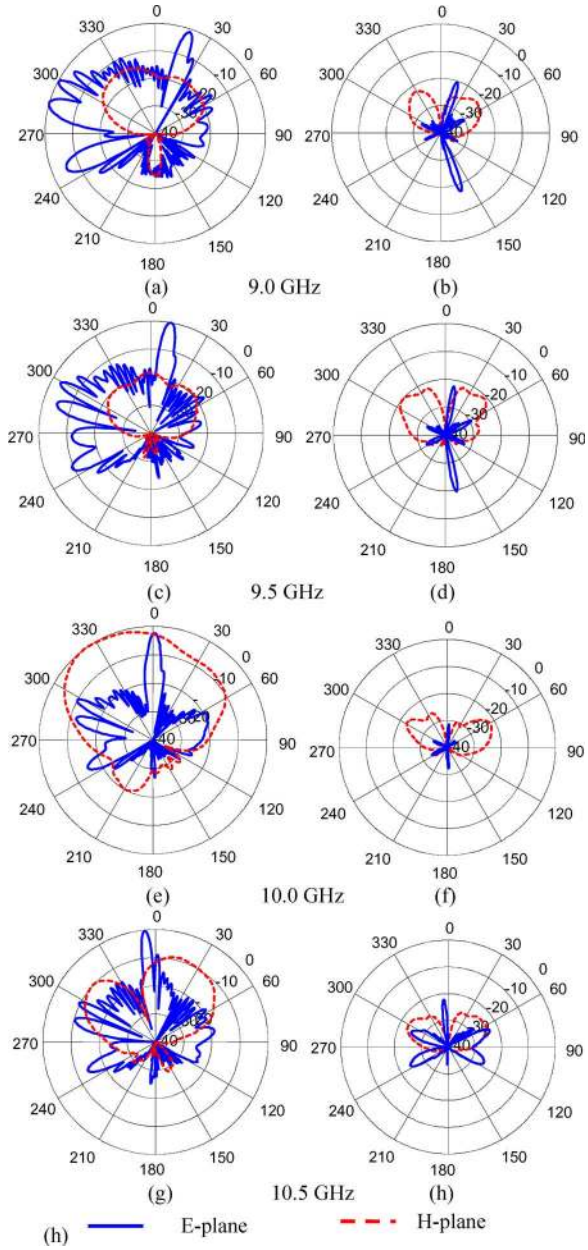

Fig. 19. Radiation patterns for the 15-element DRA array with a conducting strip around the DRA at different frequencies. The left hand side for Co-polar patterns and the right hand side for the X-polar patterns.

A. DRAs Wrapped With a Conducting Strip

Wrapping a conducting strip around the DRA is more practical and easier to implement, but it also suppresses the modes and reduces the cross polarization in a similar way as the shorting conducting plate. The following subsections show the effect of the conducting strip for the two cases discussed earlier.

1) 7-Element Array: Fig. 18 shows the simulated and measured radiation patterns at different frequencies for a 7-element

TABLE VI
SIMULATED GAIN AND RADIATION EFFICIENCY OF THE 15-ELEMENT DRA ARRAY WITH ELEMENTS WRAPPED WITH NARROW CONDUCTING STRIPS

Frequency (GHz)	η %	G_{sim} (dBi)
9.0	85.1	10.48
9.5	76.3	10.38
10.0	63.0	12.46
10.5	64.6	9.91

DRA array with DRA elements wrapped by a narrow conducting strip at its center. Compared to Fig. 14, it is noticed that the cross polarization is also reduced by about 17 dB with no changes in the co-polarization, and the reduction in the cross polarization is almost the same as using the shorting conducting plates at the center of the DRAs.

The computed and measured gains of the antenna are shown in Table V. The results are in good agreement. It can be noticed that the gain is low for the 7-element array because lots of power is transmitted to the second port, as can be noticed by comparing Fig. 10(c) to Fig. 14. Also, the simulated radiation efficiencies of the antenna are shown in the table.

2) 15-Element Array: For a 15-element DRA array with 40 dB sidelobe level with elements wrapped with narrow conducting strips, Fig. 19 shows the simulated radiation patterns at different frequencies. The cross polarization level is about 20 dB below the co-polarization level for this case.

The simulated gain and radiation efficiencies of the antenna array with conducting strips around the DRAs are shown in Table VI. At 10 GHz the gain is 12.46 dBi, while for the 7-DRA array it was 7.61 dBi. This indicates that much less power is transmitted to the second port.

VI. CONCLUSION

Linear dielectric resonator antenna arrays fed by dielectric image guide were presented. The effective dielectric constant method was used to approximate the coupling between the DIG and the DRA elements. A Dolph-Chebyshev amplitude distribution was used to control the sidelobe level of the array radiation patterns. Linear arrays of 7 and 15 elements of rectangular DRAs were designed and the cross polarization was reduced by inserting a metal sheet at the center of the DRA or by wrapping the DRA at the center by narrow conducting strip. The simulated results for the 7-element arrays were verified experimentally.

ACKNOWLEDGMENT

The support of the Department of Electrical Engineering and the Center for Applied Electromagnetic Systems Research (CAESR) at the University of Mississippi is acknowledged.

REFERENCES

[1] A. A. Kishk, "Dielectric resonator antenna, a candidate for radar applications," in *Proc. IEEE Radar Conf.*, May 2003, pp. 258–264.
[2] J. Shin, A. A. Kishk, and A. W. Glisson, "Analysis of rectangular dielectric resonator antennas excited through a slot over a finite ground plane," in *Proc. IEEE AP-S Int. Symp.*, Jul. 2000, vol. 4, pp. 2076–2079.
[3] I. A. Eshrah, A. A. Kishk, A. B. Yakovlev, and A. W. Glisson, "Theory and implementation of dielectric resonator antenna excited by a waveguide slot," *IEEE Trans. Antennas Propag.*, vol. 44, no. 53, pp. 483–494, Jan. 2005.
[4] K. M. Luk and K. W. Leung, *Dielectric Resonator Antennas*. London, U.K.: Research Studies Press, 2004.
[5] A. A. Kishk, A. Ittipiboon, Y. M. M. Antar, and M. Cuhaci, "Dielectric resonator antenna fed by a slot in the ground plane of a microstrip line," in *Proc. 8th Int. Conf. on Antennas Propag., ICAP'93, Part 1*, Apr. 1993, pp. 540–543.
[6] G. P. Junker, A. A. Kishk, and A. W. Glisson, "Input impedance of dielectric resonator antennas excited by a coaxial probe," *IEEE Trans. Antennas Propag.*, vol. 42, no. 7, pp. 960–966, Jul. 1994.
[7] R. A. Kranenberg and S. A. Long, "Microstrip transmission line excitation of dielectric resonator antennas," *IEE Electron. Lett.*, vol. 24, pp. 1156–1157, Sep. 1988.
[8] A. Al-Zoubi, A. Kishk, and A. W. Glisson, "Analysis of aperture coupled dielectric resonator antenna fed by dielectric image line," in *Proc. IEEE Antennas Propag. Society Int. Symp.*, Jul. 2006, pp. 2519–2522.
[9] A. S. Al-Zoubi, A. A. Kishk, and A. W. Glisson, "Analysis and design of a rectangular dielectric resonator antenna fed by dielectric image line through narrow slots," *Progr. Electromagn. Res.*, vol. PIER 77, pp. 379–390, 2007.
[10] A. Al-Zoubi, A. Kishk, and A. Glisson, "Slot-aperture-coupled linear dielectric resonator array fed by dielectric image line backed by a reflector," in *Proc. IEEE Antennas Propag. Society Int. Symp.*, Jul. 2008, pp. 1–4.
[11] S. Shindo and T. Itanami, "Low-loss rectangular dielectric image line for millimeter-wave integrated circuits," *IEEE Trans. Antennas Propag.*, vol. 26, no. 10, pp. 747–751, Oct. 1978.
[12] K. Solbach and I. Wolff, "The electromagnetic fields and the phase constants of dielectric image lines," *IEEE Trans. Antennas Propag.*, vol. 26, no. 4, pp. 266–274, Apr. 1978.
[13] F. Farzaneh, P. Guillon, and Y. Garault, "Coupling between a dielectric image guide and a dielectric resonator," in *Proc. IEEE MTT-Digest*, 1984, pp. 115–117.
[14] M. T. Birand and R. V. Gelsthorpe, "Experimental millimetric array using dielectric radiators fed by means of dielectric waveguides," *Electron. Lett.*, vol. 17, pp. 633–635, Sep. 1981.
[15] R. M. Knox and P. P. Toulios, "Integrated circuits for the millimeter through optical frequency range," in *Proc. Symp. Submillimeter Waves*, 1970, pp. 497–516.
[16] P. Bhartia and I. J. Bahl, *Millimeter-Wave Engineering and Application*. New York: Wiley, 1984.
[17] HFSS: High Frequency Structure Simulator Based on Finite Element Method11.0.2 ed. Ansoft Corporation, 2007.
[18] M. W. Wyville, "Dielectric resonator antenna arrays in the EHF band," Master's thesis, Carleton University, Dept. Electron., Ottawa, ON, Canada, 2005.
[19] M. W. Wyville, A. Petosa, and J. S. Wight, "DIG feed for DRA arrays," in *Proc. IEEE Antennas Propag. Society Int. Symp.*, Jul. 2005, pp. 176–179.
[20] A. S. Al-Zoubi, "Rectangular dielectric resonator antennas fed by dielectric image guides," Ph.D. dissertation, Univ. Mississippi, Dept. Elect. Eng., University, 2008.
[21] T. K. Tam and R. D. Murch, "Half volume dielectric resonator antenna," *Electron. Lett.*, vol. 33, no. 23, pp. 1914–1916, Nov. 1997.

Asem S. Al-Zoubi (M'09) received the B.Sc. degree from Eastern Mediterranean University, Cyprus, in 1993, the M.Sc. degree from Jordan University of Science and Technology, in 1998, and the Ph.D. degree from the University of Mississippi, University, in 2008, all in electrical engineering.

Currently, he is an Assistant Professor with the Department of Communications Engineering in Al-Yarmouk University, Jordan. From October 1999 to October 2000, he worked as a Laboratory Supervisor at Princess Sumaya University for Technology (PSUT), Jordan. From October 2000 to January 2004, he worked as a Lecturer in the Telecommunication Department, Institute of Science for Telecom and Technology, Riyadh, Saudi Arabia. His current research interests include dielectric resonator antennas and microstrip antennas.

Dr. Al-Zoubi is a member of the Sigma Xi Society.

Ahmed A. Kishk (S'84–M'86–SM'90–F'98) received the B.S. degree in electronic and communication engineering from Cairo University, Cairo, Egypt, in 1977, the B.S. degree in applied mathematics from Ain-Shams University, Cairo, Egypt, in 1980, and the M.Eng. and Ph.D. degrees from the University of Manitoba, Winnipeg, MB, Canada, in 1983 and 1986, respectively.

He has been a Professor of electrical engineering at the University of Mississippi, University, since 1995. He has published over 200 journal articles and book chapters.

Prof. Kishk was an Editor-in-Chief of the *ACES Journal* from 1998 to 2001 and has been an Editor of the *IEEE Antennas and Propagation Magazine* since 1993. He received the 1995 and 2006 *ACES Journal* outstanding paper awards, and the Microwave Theory and Techniques Society Microwave Prize in 2004.

Allen W. Glisson (S'71–M'78–SM'88–F'02) received the B.S., M.S., and Ph.D. degrees in electrical engineering from the University of Mississippi, University, in 1973, 1975, and 1978, respectively.

In 1978, he joined the faculty of the University of Mississippi where he is currently Professor and Chair of the Department of Electrical Engineering. His current research interests include the development and application of numerical techniques for treating electromagnetic radiation and scattering problems, and modeling of dielectric resonators and dielectric resonator antennas.

Dr. Glisson is a Fellow of the IEEE, a Fellow of the Applied Computational Electromagnetics Society, and a member of Commission B of the International Union of Radio Science. He received a Best Paper Award from the SUMMA Foundation and twice received a citation for Excellence in Refereeing from the American Geophysical Union. He was a recipient of the 2004 Microwave Prize awarded by the Microwave Theory and Techniques Society and received the 2006 Best Paper Award from the *Applied Computational Electromagnetics Society Journal*. He was selected as the Outstanding Engineering Faculty Member in 1986, 1996, and 2004. He received a Ralph R. Teetor Educational Award in 1989 and in 2002 he received the Faculty Service Award in the School of Engineering. He served as the Associate Editor for Book Reviews and Abstracts for the *IEEE Antennas and Propagation Magazine* from 1984 until 2006. He currently serves on the Board of Directors of the Applied Computational Electromagnetics Society, is Treasurer of the society, and is a member of the AP-S IEEE Press Liaison Committee. He has previously served as a member of the IEEE Antennas and Propagation Society Administrative Committee, as the secretary of Commission B of the U.S. National Committee of URSI, as an Associate Editor for *Radio Science*, as Co-Editor-in-Chief of the *Applied Computational Electromagnetics Society Journal*, and as the Editor-in-Chief of the IEEE TRANSACTIONS ON ANTENNAS AND PROPAGATION.